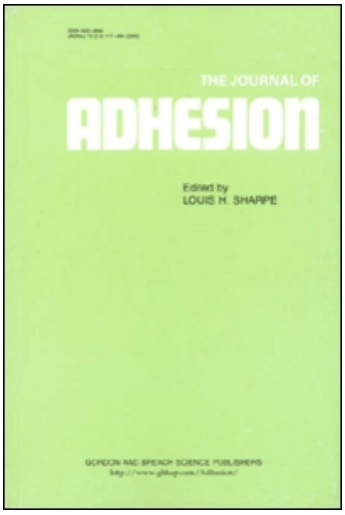

The Journal of Adhesion
Publication details, including instructions for authors and subscription information:
http://www.informaworld.com/smpp/title~content=t713453635

Contact Angle Hysteresis: The Need for New Theoretical and Experimental Models

E. L. Decker[a]; S. Garoff[a]
[a] Department of Physics and Colloids, Polymers, and Surfaces Program, Carnegie Mellon University, Pittsburgh, PA, USA

To cite this Article Decker, E. L. and Garoff, S.(1997) 'Contact Angle Hysteresis: The Need for New Theoretical and Experimental Models', The Journal of Adhesion, 63: 1, 159 — 185
To link to this Article: DOI: 10.1080/00218469708015219
URL: http://dx.doi.org/10.1080/00218469708015219

J. Adhesion, 1997, Vol. 63, pp. 159–185
Reprints available directly from the publisher
Photocopying permitted by license only

Contact Angle Hysteresis: The Need for New Theoretical and Experimental Models*

E. L. DECKER and S. GAROFF**

Department of Physics and Colloids, Polymers, and Surfaces Program, Carnegie Mellon University, Pittsburgh, PA 15213, USA

(Received 28 June 1996; In final form 30 September 1996)

Wetting on ambient, heterogeneous surfaces is characterized by contact angle hysteresis. Quantitative models of contact angle hysteresis are essential in order to design surfaces with specific wetting behavior or to interpret experiments seeking to characterize a surface through its wetting properties. We focus on the successes and failures of theoretical models as well as experiments on model surfaces in describing contact angle hysteresis on ambient surfaces. We describe experimental observations of contact line structure and dynamics as well as contact angle hysteresis on laboratory surfaces. We discuss three general classes of models treating one-dimensional periodic heterogeneity, two-dimensional periodic heterogeneity, and random heterogeneity. We show where these models succeed and where they fail to agree quantitatively and qualitatively with experimental observations. New models treating strong, dense heterogeneity as well as temporal relaxation of contact angles in experimental environments need to be developed to provide quantitative descriptions of contact angle hysteresis on ambient surfaces.

Keywords: Contact angle; contact angle hysteresis; wetting; spreading; heterogeneous surface; contact line; interface roughness

1. INTRODUCTION

The quantitative description of wetting of ambient surfaces is important in many industrial and scientific areas [1–3]. The contact angle of

*One of a Collection of papers honoring Robert J. Good, the recipient in February 1996 of *The Adhesion Society Award for Excellence in Adhesion Science, sponsored by 3M.*

**Corresponding author.

liquids on solid surfaces is a measure of the wetting characteristics of the surfaces. However, contact angle measurement on ambient surfaces has inherent uncertainty. The local contact angle varies spatially across the surface. In addition, the macroscopically-averaged contact angle can take on a range of values between two fairly reproducible extremes: the advance and the recede contact angles. For instance, if a liquid drop is placed on a solid surface and the solid is then tilted from the horizontal, the drop takes on an asymmetric shape when viewed from the side. The macroscopically-averaged contact angle within the liquid, measured between the solid and the liquid-vapor interface of the drop, is larger at the lower end of the drop than at the higher end. If the surface is tilted further, the maximum angle attained at the lower end of the drop just before the drop begins to roll is the macroscopically-averaged advance contact angle. Similarly, the minimum angle attained at the higher end of the drop just before the drop rolls is the macroscopically-averaged recede contact angle. Even these fairly reproducible, extreme contact angles (advance and recede) depend on factors other than just the three materials (solid, liquid and vapor) involved. For instance, the time scale of the measurement process and the vibration level of the environment can influence the measured angles [4–6]. The disparity between the macroscopically-averaged advance and recede contact angles is called contact angle hysteresis. Contact angle hysteresis influences many wetting phenomena on ambient surfaces, such as the ability of liquid drops to be retained or shed from surfaces [7–9] or the movement of liquids through porous media [10]. Even though qualitative characteristics of contact angle hysteresis have long been recognized, a quantitative description has not yet been achieved. Such a description is necessary in order to define the level of homogeneity needed to remove hysteresis, to design a system with controlled hysteresis, or to make full use of contact angle measurements as a diagnostic of a surface.

In this paper, we focus on the successes and failures of theoretical models as well as experiments on model surfaces in describing contact angle hysteresis on ambient surfaces. We have not written an exhaustive review of the literature. In the remainder of the introduction, we examine fundamental ideas such as the correct definition of contact angles on ambient surfaces, the role of dissipation in hysteresis, and the microscopic and macroscopic behavior of a contact line (CL) as it

moves across an ambient surface. Next, we present a description and some experimental realizations of ambient surfaces. We describe experimental observations of CL structure and dynamics, as well as contact angle hysteresis, on these surfaces. We then examine models of hysteresis on three classes of heterogeneous surfaces with one-dimensional (1D) periodic heterogeneity, two-dimensional (2D) periodic heterogeneity, or random heterogeneity. The 1D models basically show how metastable states can arise from chemical heterogeneity and can thus produce hysteresis. The 2D models go a step further by examining the broken structure of the CL. The random models attempt to provide a description of real ambient surfaces. Finally, we discuss the effects of vibrations on temporal relaxation of contact angles.

Chemical heterogeneity and physical roughness of surfaces are accepted origins of contact angle hysteresis [1,11–14]. We examine hysteresis due to these surface characteristics and limit our discussion to systems in which all of the interfacial energies are static on the time scale of experiments. In addition, we are not treating hysteresis due to penetration of the liquid into the intermolecular pores of the solid [15] or "intrinsic" sources [16, 17].

1.1. Definition of Contact Angles

A useful geometry for studying contact angle hysteresis is the Wilhelmy plate geometry, a vertical plate which is partially immersed in a container of liquid (Fig. 1) [18]. In any geometry, the CL is the locus of points where the solid, liquid, and vapor phases meet. In the Wilhelmy plate geometry, the height, h, of the CL (averaged over a macroscopic length of the CL) relative to the bulk liquid level is related to the macroscopically-averaged contact angle, θ, by [19]

$$h = 2a\sin(45^\circ - (\theta/2)) \tag{1}$$

where $a = \gamma_{LV}/(\Delta\rho g)$ is the capillary length, $\Delta\rho$ is the density difference between the liquid and the vapor, g is the acceleration of gravity, and γ_{LV} is the liquid-vapor interfacial energy. If a plate with an ambient surface is slowly pulled out of the liquid, h increases to a maximum value of h_r, the macroscopically-averaged recede rise height. Similarly, if the plate is pushed into the liquid, the rise height decreases to a minimum value of h_a, the macroscopically-averaged advance rise

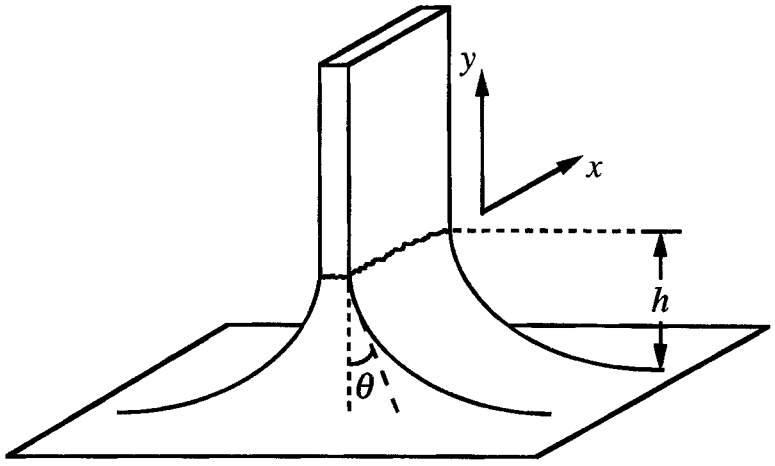

FIGURE 1 Wilhelmy plate geometry of a partially-immersed, vertical plate. h = rise height. θ = contact angle.

height. These extreme heights h_r and h_a are, respectively, related to the macroscopically-averaged contact angles θ_r and θ_a by Eq. (1). Unless explicitly stated otherwise, we will use the Wilhelmy plate geometry for our discussion of contact angles and hysteresis.

To determine the wettability of a surface one often uses contact angle measurement [18]. We can describe contact angles in terms of local values and macroscopically-averaged values. In either case, the contact angle is the boundary condition to the Laplace equation, which predicts the shape of the liquid-vapor interface [13].

$$\Delta P = \Delta\rho g f = \gamma_{LV}\left(\frac{1}{R_1} + \frac{1}{R_2}\right) \tag{2}$$

where ΔP is the pressure difference across the liquid-vapor interface as a function of position on the interface, f is the local height of the liquid-vapor interface relative to the bulk liquid level where the liquid-vapor interface is flat, and R_1 and R_2 are the local principal radii of curvature of the interface. Local and macroscopically-averaged contact angles may be approximated by tangents to the liquid-vapor interface at the solid surface (looking at the meniscus from the side). However, such a measurement is magnification dependent, *i.e.*, it depends on how close to the CL a tangent is placed. Correct contact angles are found by

considering the behavior of the liquid-vapor interface some distance from the solid and extrapolating to the solid surface. This latter, correct method, is equivalent to measuring the rise height on a local length scale for a local angle, or on a macroscopic length scale for a macroscopic angle (looking directly at the CL – not from the side) and using Eq. (1).

For ambient surfaces, the local rise height, and thus the local contact angle, varies across the surface. Thus, for the purpose of examining the local fluctuations in the wettability of the solid surface and the resulting morphology of the liquid-vapor interface, the CL should be microscopically imaged with high magnification. By this method, the local contact angles will be measured over a very short length scale.

If one wishes to obtain only the average wetting characteristics of the solid surface rather than a precise mapping of the local wettability, a macroscopically-averaged contact angle is needed. The variations in the liquid-vapor interface due to a rough CL diminish over short distances away from the CL [20, 21]. In the Wilhelmy plate geometry, sufficiently far from the CL the curvature of the interface parallel to the plate becomes negligible compared with the curvature perpendicular to the plate. The macroscopically-averaged contact angle is the boundary condition for the extrapolation of this smooth liquid-vapor interface to the solid. To obtain this macroscopic boundary condition, the contact angle should be averaged over a sufficiently large length scale. Thus, the use of the contact angle dictates which length scale to consider.

At length scales larger than the capillary length, gravitational forces may dominate and flatten the CL. The rise height may become constant when averaged on such scales and a macroscopically-averaged contact angle can be obtained from the rise height averaged over several capillary lengths using Eq. (1). As we shall see, the CL may show significant distortions over length scales much larger than the capillary length. In such cases, it makes no sense to report a single contact angle for the surface. These considerations must be taken into account when measuring contact angles on sessile drops where the largest length scale of the measurement is set by the perimeter of the drop.

1.2. Contact Angle Hysteresis

Hysteretic systems are trapped in metastable states which depend on the history of the system. They dissipate energy if they are forced to

traverse slowly from one state to another. The origins of macroscopic contact angle hysteresis lie in the distortions and dynamics of local portions of the contact line. Microscopically, the local contact angle varies spatially across the surface in an attempt to conform to the local wettability and/or geometry of the surface. Thus, the CL will be uneven as it becomes locally distorted by the surface heterogeneities. If the system is static, no net force can be acting on each point on the CL. Each point on the CL is in a metastable state, *i.e.*, a state of local – but not necessarily global – minimum of energy. (Many types of hysteresis are thought to arise from the existence of microscopic domains of a system that are caught in metastable states [22–24]). As the bulk liquid slowly moves relative to the solid (*e.g.*, by raising or lowering the plate in the fluid bath), a local variation of the wettability of the surface can pin a portion of the CL and stretch it from the average CL position. When the stretch of the liquid-vapor interface becomes too great (the elastic force of the stretched liquid-vapor interface becomes greater than the force of the wettability pinning the microscopic section of the CL), the distorted section of the CL quickly snaps to a less stretched configuration. In the snapping process, energy is thermally dissipated. In addition to the energy dissipation of the snapping motion, energy is also dissipated in the fluid due to the slow, forced motion of the plate. However, unlike the dissipation in the snaps, the continuous dissipation due to the forced plate motion tends toward zero as the plate motion is slowed. This dissipation of energy, even in the limit of zero forced motion, is characteristic of a hysteretic system. For contact angle hysteresis, the regime of motion where the energy dissipation in microscopic jumps dominates the dissipation due to the forced motion is called quasistatic motion.

We can connect the energy discussion above to the notion of history-dependent states of the system. If the CL microscopically distorts during slow, forced motion, but smoothly reconfigures without snapping, then the only dissipation in the system is due to the forced motion of the bulk liquid. No hysteresis should be present. In fact, Joanny and de Gennes [20] have shown that the CL snaps only if distortions are history-dependent (*i.e.* only if the microscopic distortion depends on the direction of motion of the liquid relative to the solid). While their argument focuses on a single defect, a similar argument could be formulated for cooperative pinning of the CL by collections of defects.

Macroscopically, hysteresis is the result of the combined effect of the microscopic distortions and snaps. Consider a vertical plate with an ambient surface being quasistatically (*i.e.*, at a slow enough velocity so that the steady viscous dissipation due to forced motion is negligible) pushed into and pulled out of the liquid. As the downward motion begins, the CL is microscopically pinned; and thus the macroscopically-averaged contact angle increases. As the liquid-vapor interface locally stretches and applies an increasing force to the microscopically-pinned portions of the CL, some of the microscopic portions of the CL snap. The snaps occur with increasing frequency as the elastic force overcomes the pinning force of more and more local sections of the CL. At some point, continually occurring microscopic jumps along the CL prevent the macroscopically-averaged rise height from decreasing further. The macroscopic contact angle has reached its advance value. During the upward half of the cycle, a similar process lets the macroscopically-averaged rise height increase but microscopic snaps prevent the macroscopically-averaged contact angle from moving beyond the recede angle. If the forcing of the system is stopped at any point in this cycle, the macroscopically-averaged contact angle will be somewhere between the advance and recede angle. The metastable states trapping the microscopic portions of the CL produce a range of macroscopically-averaged contact angles with a maximum (advance) and minimum (recede) value. Thus, the macroscopic hysteresis is directly related to the mechanics of the pinning of microscopic portions of the CL. In addition, since the dissipation due to the forced motion of the bulk liquid becomes negligible in the quasistatic regime, the total macroscopic energy dissipation in quasistatically moving around the hysteresis loop described above is the sum of the energy irreversibly dissipated in all of the microscopic jumps.

2. AMBIENT SURFACES

2.1. Description

We consider smooth but chemically heterogeneous surfaces (*e.g.* smooth ambient surfaces which have become contaminated). Modeling of hysteresis due to surface roughness is mathematically similar to that for chemical heterogeneity [20]. Hence, our discussion could apply to

rough ambient surfaces, as long as the surface roughness does not promote wicking of the liquid along surface roughness features (thus causing the local CL to be far removed from the macroscopically-averaged CL).

The total energy of the system dictates the structure and quasistatic behavior of a CL on an ambient surface. The three components of that energy are: gravitational potential of the fluid in the meniscus, interfacial energy of the liquid-vapour interface (γ_{LV} is the energy per unit area of this interface), and the energy of the liquid or vapor in contact with the solid surface (γ_{SV} and γ_{SL} are, respectively, the energy per unit area of the solid-vapor and solid-liquid interfaces). For an ambient surface with spatially varying wettability, γ_{SV} and γ_{SL} will depend on the position on the solid. To find the contribution to the total energy from the wettability of the solid, we need the difference of γ_{SL} from γ_{SV} as a function of position on the solid. We will define the wettability function to be

$$c(\mathbf{r}) = [\gamma_{SV}(\mathbf{r}) - \gamma_{SL}(\mathbf{r})]/\gamma_{LV} \tag{3}$$

where $\mathbf{r}$ represents the spatial coordinates in the plane of the surface. The wettability function, $c(\mathbf{r})$, could be equated to the cosine of the local contact angle, $\cos\theta(\mathbf{r})$, if we were to assume validity of Young's equation ($\gamma_{SV} - \gamma_{SL} = \gamma_{LV}\cos\theta$). The use of the wettability function in Eq. (3) to carry out an energy minimization to find the locally stable configurations of the CL assumes that γ_{SV} and γ_{SL} are evaluated only at the locus of $\mathbf{r}$ values along the CL. However, thermal fluctuations and/or mechanical vibrations cause the CL to sample some small region along the surface. Thus, the force balance or variational description of the energy must consider the wettability function at least over such regions. This issue must be carefully addressed when the CL is near a rapid spatial variation of the surface properties, such as near a physical edge, the edge of a microfabricated wettability pattern [25, 26], or natural wettability boundaries formed by the spreading of complex fluids [27, 28].

The wettability function in Eq. (3) may be written

$$c(\mathbf{r}) = c_0 + c_f(\mathbf{r}) \tag{4}$$

where c_0 is the average wettability of the surface,

$$c_0 = \int_{\text{all r in surface}} c(\mathbf{r})d\mathbf{r} \Big/ \int_{\text{all r in surface}} d\mathbf{r} \tag{5}$$

and $c_f(\mathbf{r})$ maps the spatial fluctuations of the wettability from the average. If c were to be equated to the cosine of the contact angle, then c_0 would represent the Cassie angle [29].

For a truly random (and physically unattainable) surface, $c_f(\mathbf{r})$ would have no spatial correlations, *i.e.*

$$\langle c_f(\mathbf{r})c_f(\mathbf{r}')\rangle \propto \delta(\mathbf{r}-\mathbf{r}') \tag{6}$$

In this case, there would be no characteristic length scale for the surface heterogeneity. For a real ambient surface, there will be some correlation over short distances (minimally at molecular sizes). Such correlations are sometimes modeled with a Gaussian correlation function

$$\langle c_f(\mathbf{r})c_f(\mathbf{r}')\rangle \propto \exp(-|\mathbf{r}-\mathbf{r}'|^2/d^2) \tag{7}$$

where d is a length scale characterizing the decay of the spatial correlations [30].

If an ambient surface is modeled as randomly placed localized defects, then two characteristic lengths arise: the correlation length (defect size) and the average distance between defects. However, if the defect density increases until the defects overlap significantly, then the surface can again be characterized by a single correlation length. This single length scale, which describes the correlation of the heterogeneity of the wettability function, we will also call the "heterogeneity size". We will focus on surfaces where the heterogeneity size is much less than the capillary length.

2.2. Observations

Experimental Models of Ambient Surfaces: Models of natural ambient surfaces have been created by degradation of a uniform surfactant

monolayer, by formation of an incomplete surfactant monolayer, by formation of a mixed surfactant monolayer, or by deposition of defect spots on a smooth substrate. In our lab, we often use degradation by ultraviolet (UV) irradiation of a full monolayer of Aquapel^{TM} on a smooth glass substrate. We can produce surfaces of varying heterogeneity by varying the UV irradiation time. We have done preliminary examination of the heterogeneity size on such surfaces using optical ellipsometry, x-ray reflectivity, and atomic force microscopy measurements. These characterization techniques suggest that the heterogeneity formed by the UV degradation is probably of molecular or supermolecular (but submicroscopic) lateral scale (perhaps ~ 100Å). Since these methods do not examine the surface on all length scales which may be relevant to wetting, it is difficult to obtain conclusive evidence of the surface characteristics from them. In addition, surface chemistry variations, far too subtle to be detected by these techniques, can affect wetting significantly.

Other ambient surfaces have been made by formation of an incomplete surfactant monolayer on a smooth substrate [12, 31]. In one case, patches of TiO_2 on glass prevent the formation of a full monolayer of an ionic surfactant [12]. In another case, a film of silver was exposed to varying amounts of an alkanethiol surfactant [31]. The result in both cases was a surface with both a high energy component and a low energy component with varying surface coverage.

Many ambient surfaces have been created by formation of mixed self-assembled monolayers (SAMs) of alkanethiols with different end groups at the air-monolayer interface [32–36]. Several studies of wetting on two-component SAMs have inferred or assumed the heterogeneity of these surfaces to be of molecular scale [33–35]. However, scanning tunneling microscopy done on two-component SAMs has shown the SAMs can phase separate into single-component regions of the order of 10–100Å [36].

Surfaces with randomly placed defects have been produced to simulate random surfaces experimentally [5, 37]. In such cases, spots of one wettability are drawn on a substrate of another wettability. Such surfaces have features which may not replicate important characteristics of ambient surfaces: the defects may not be small compared with the capillary length and the surfaces are dominated by one-size heterogeneity. Analysis of such surfaces must account for the fact that the

spots themselves, as well as the backing substrate, often exhibit contact angle hysteresis.

CL Roughness: Competing forces give rise to CL structure. The heterogeneity distorts the CL and pins sections of the CL so that they stretch hysteretically. Surface tension competes with these pinning forces to bring the CL distortions to less-stretched configurations. On length scales much smaller than the capillary length, gravitational forces will be smaller than surface tension. Thus, on these scales pinning forces compete primarily with surface tension. On some length scale greater than the capillary length, gravity should dominate all the forces and prevent increasing CL roughness on larger scales.

We have examined features of CLs of water on our degraded-monolayer ambient surfaces in the Wilhelmy plate geometry. The techniques we used have been described elsewhere [6]. We observe CL roughness at our highest resolution, on the order of 1μm (Fig. 2). We observe CLs which are flat on length scales comparable to the capillary length (Fig. 3a). However, we often observe CL distortions over length scales longer than the capillary length of 2.7 mm (Fig. 4a).

To examine more clearly the length scales over which the various forces compete to give the observed CL roughness, we calculate the root mean square (rms) CL width, w, *versus* averaging length, L. For a

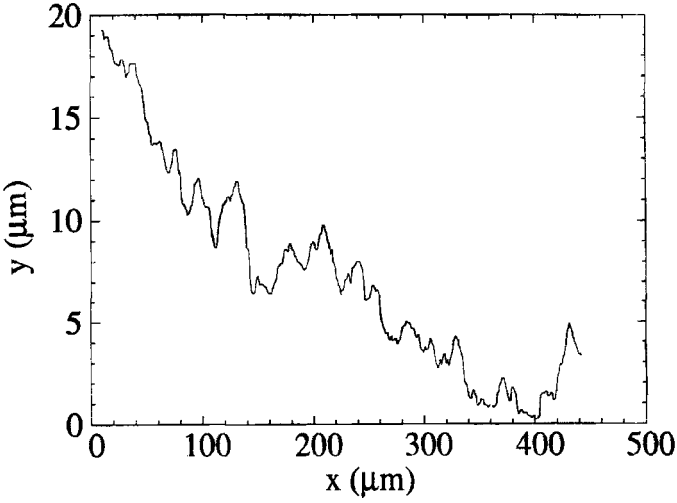

FIGURE 2 Highly magnified CL configuration.

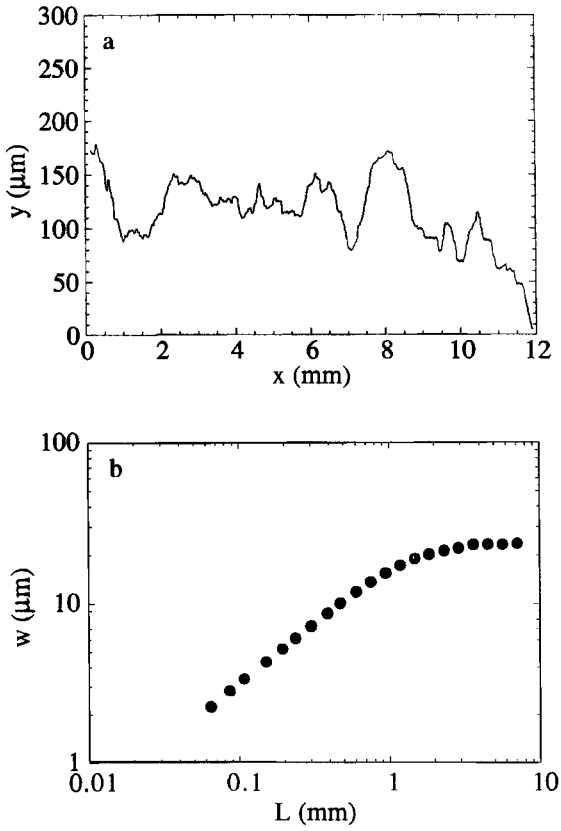

FIGURE 3 a) CL configuration with distortions extending only over lengths less than the capillary length (2.7 mm). b) Corresponding plot of rms CL roughness, w, *versus* averaging length scale, L.

CL given by $y(x)$ of total length D, the rms CL width is

$$w(L) = \left\{ \frac{1}{D-L} \int_{-(D-L)/2}^{(D-L)/2} \sigma_L^2(x_0) dx_0 \right\}^{1/2} \tag{8}$$

with

$$\sigma_L^2(x_0) = \frac{1}{L} \int_{x_0-(L/2)}^{x_0+(L/2)} [y(x) - \bar{y}_L(x_0)]^2 dx \tag{9}$$

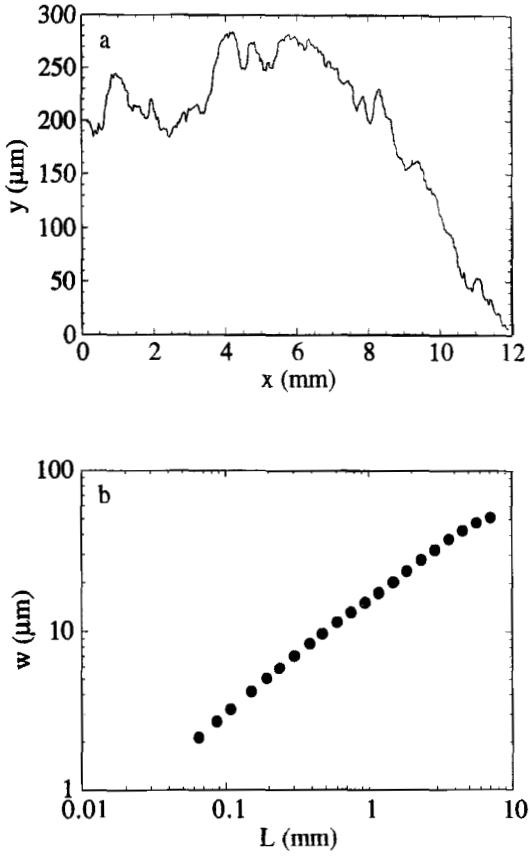

FIGURE 4 a) CL configuration with distortions extending over length scales larger than the capillary length (2.7 mm). b) Corresponding plot of rms CL roughness, w, *versus* averaging length scale, L.

$$\bar{y}_L(x_0) = \frac{1}{L}\int_{x_0-(L/2)}^{x_0+(L/2)} y(x)dx \tag{10}$$

Two examples of w *versus* L plots are shown in Figures 3b and 4b. These plots correspond to the CL configurations in Figures 3a and 4a, respectively. In Figure 3b the curve turns over roughly at the capillary length of water. However, at a different location on the same surface the CL roughness continues to increase up to at least three times the capillary length (Fig. 4b). Thus, pinning forces can be large enough to

compete with gravity to large lengths even on surfaces where we believe the length scale of the chemical variations is much smaller.

A plot of ensemble-averaged *w versus L* from ten CL configurations from one surface is shown in Figure 5. Below the gravitational turn over, *w versus L* is roughly a power law. The exponent of a forced power law fit in this region is 0.76. We have observed exponents of 0.66 to 0.87 for ensembles of CLs on our experimental ambient surfaces.

Hysteresis Versus Surface Coverage: The dependence of hysteresis on the amount of heterogeneity (surface coverage of different wettability components) is the most common measurement made on model surfaces. This dependence, as well as the dependence of the advance and recede angles, is qualitatively very different for various experimental surfaces whether produced by defected or mixed monolayers [12, 31, 33, 34]. For surfaces produced with random dots, hysteresis was not measured *versus* surface coverage, but rather *versus* defect number density [37]. The results are again qualitatively different from those of the other model surfaces. For the random-dot model, two regimes are seen in the data: one for non-interacting (widely spaced) defects and one for interacting defects. A power law dependence of the hysteresis on the density of interacting defects is observed.

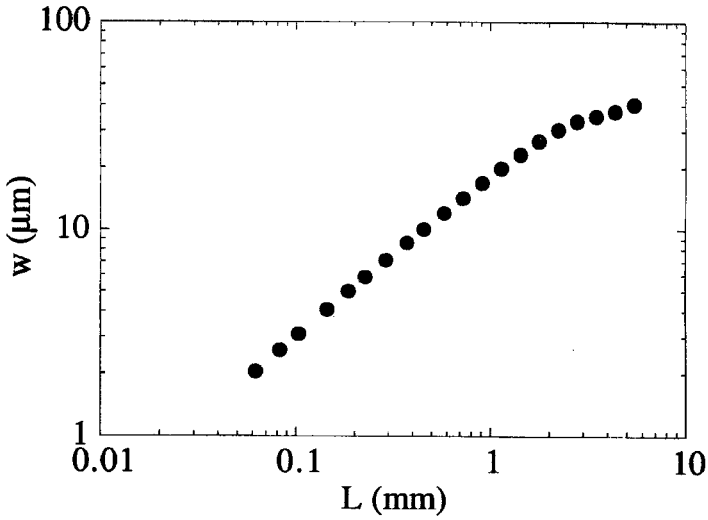

FIGURE 5 Ensemble-averaged rms CL roughness, *w*, *versus* averaging length scale, *L*, for ten CL configurations on one surface.

CL Jumps: We have observed CL dynamics for slow motion of our degraded monolayer surfaces into or out of a beaker of water. The microscopic jumps of the CL are very complex. We have observed jumps ranging in size from about 1 mm in extent along the CL and about 100 μm perpendicular to the CL down to about micron scale in both directions. The relaxation of one section of the CL can induce relaxation of another section. Thus, some correlation in the jumps is seen. In spite of the complex nature of the jumps, a high degree of reproducibility has been seen in CL configurations for multiple cycles of a solid into and out of a liquid [6, 38].

3. QUASISTATIC MODELS OF HYSTERESIS

3.1. One-Dimensional Periodic Heterogeneity

The first models of hysteresis examined surfaces with one-dimensional (1D) periodic variation of the wettability and unbroken contact lines parallel to the wettability variation [12, 13, 39–41]. Even though a 1D wettability pattern is not physically descriptive of an ambient surface, 1D models are useful for examining the relation between heterogeneity and hysteresis. There are three components to the energy of such a system: gravity, the elastic energy in the stretched liquid-vapor interface, and the solid surface wettability. To determine the behavior of the system, the total energy functional per unit length is minimized against variations in the contact line position. The 1D models all exhibit metastable minima with energy barriers. All the models predict hysteresis with a maximum (advance) contact angle and a minimum (recede) contact angle. Thus, these models successfully show the qualitative existence of hysteresis and pinning of the CL in metastable states due to heterogeneity. Even though these models are useful for showing the origin of metastable states that produce hysteresis in wetting systems, they are limited in their ability to model ambient surfaces.

CL Roughness: When considering static CLs, all the 1D models consider only an unbroken CL parallel to the heterogeneity boundaries. The elastic energy stored in the distortions of the liquid-vapor interface which accompanies a rough CL is neglected. As we shall see, this

energy is essential in accounting for hysteresis on ambient surfaces. Obviously, these models do not attempt to account for the roughness of CLs observed on ambient surfaces.

Hysteresis Versus Surface Coverage: One-dimensional models in the Wilhelmy plate geometry (vertical plate hanging in liquid) treat solid surfaces with horizontal stripes of different homogeneous wettability [13,39,40]. In a zero-vibration environment, these models predict that the hysteresis has a value that is independent of the relative stripe widths. For the addition of any stripe of a second material, the recede angle attains the same value as the contact angle on a surface with only the high energy component and the advance angle attains the same value as the contact angle on a surface with only the low energy component. Thus, the hysteresis is dependent only on the wettabilities of the two types of stripes and not on the relative coverage of the two materials. However, ambient surfaces show dependence of the hysteresis on surface coverage. Further, 1D models predict no hysteresis on striped surfaces where the pattern is tilted, even infinitesimally, relative to the contact line.

Including the effects of vibrations mitigates some of this unphysical behavior of 1D models. If vibrations can overcome the energy barriers of the 1D models, the hysteresis would be somewhat reduced [12,39–41]. Interactions of vibrations with the local energy barriers cause a dependence of the hysteresis on the ratio of stripe widths (different surface coverage) [40].

CL Jumps: In 1D periodic models, motion of the CL is predicted to be unsteady as the CL breaks free of a wettability boundary and repins at the next one. For quasistatic motion and in the presence of vibrations, the CL may depin in a wave type fashion [39]. Part of the CL may be instantaneously pinned on a lower wettability boundary with the rest of the CL pinned on a higher boundary. The kink in the CL connecting these two parts of the CL will slide along the wettability boundary in the process of depinning. These dynamics of the 1D models do not describe the unsteady motion of pinning and jumping observed for CLs on ambient surfaces. CL jumps are very complex, showing correlations between the jumping of neighboring points along the CL. The CL does not depin as a whole or as a wave.

Thus, these early 1D periodic models are useful for qualitatively demonstrating the pinning of the CL on the boundaries between regions of

different wettability. This pinning of the CL in metastable states leads to hysteresis. The interaction of vibrations with the energy barriers is predicted to be a factor in determining the amount of hysteresis. However, the magnitude of the predicted hysteresis is unphysical. In addition, these models cannot describe the structure or dynamics of CLs on ambient surfaces.

3.2. Two-Dimensional Periodic Heterogeneity

Models with a two-dimensional (2D) periodic wettability function of two wettability components were developed to mimic better the patchy heterogeneity of ambient surfaces [21,42]. The 2D models allow CL brokeness and jumps of segments of the CL. Thus, they can examine structure and dynamics of CLs not seen in 1D models. The 2D models examine the same energy contributions as the 1D models: gravity, the elastic energy in the stretched liquid-vapor interface, and the solid surface wettability. However, within these contributions is the additional energy of the brokenness of the CL. One discussion employs Fourier decomposition of the CL and the wettability function. It has a series of three ever more accurate solutions for the minimization of the energy, the range of hysteresis, and the CL configurations for a given 2D wettability pattern [21]. This model assumes that the liquid-vapor interface slope is small compared with 1 everywhere on the interface. This assumption, common in 2D and other models, simplifies the integrals representing the energy arising from the stretched liquid-vapor interface. This assumption is valid except for macroscopically-averaged contact angles near 0° or 180°. However, in terms of the variations of the local contact angle from the macroscopically-averaged angle, this assumption is much more restrictive. Further, the model assumes that the distortions of the CL from the average CL position are much smaller than the fundamental wavelength of the heterogeneity parallel to the CL. Finally, the model assumes that the fundamental wavelength in the CL is the same as that of the wettability function parallel to the CL. Thus, the broken CL in the 2D model exhibits one dominant length scale with artificially high spatial correlations.

The same Fourier decomposition technique could be extended to ambient surfaces. (This is discussed further in Section 3.3). The fundamental wavelength of the wettability pattern to be matched by the CL in this case would have to increase to the sample size. If no other

assumptions of the model [21] are violated for a given random wettability function, the mathematical structure of the model should correctly predict the CL configurations and the hysteresis on ambient surfaces where the wettability function is known.

CL Roughness: While 2D models come closer to describing the roughness of CLs on ambient surfaces, the CL structure in 2D models has an infinite correlation length. In fact, when a surface is microfabricated with 2D periodic wettability, this correlated structure of the CL has been observed [43,44]. The CL deforms due to a periodic array of patches and mimics the periodicity of the patches (Fig. 6). The shape of the periodic CL deformation depends on the patch shape and the wettability contrast between the patches and the background. In applying the general mathematical structure of 2D models to ambient surfaces, the assumptions of the model discussed in the previous section limit the validity of the model to CL distortions of very small amplitude. However, our observations on ambient surfaces indicate that the CL distortions are large compared with the assumed supermolecular scale of the heterogeneity.

Hysteresis Versus Surface Coverage: The 2D models show that hysteresis is dominated by any modulation of the wettability averaged perpendicular to the CL [21]. This modulation is reminiscent of the 1D models and is not present on ambient surfaces. If the wettability averaged perpendicular to the CL has no modulation, hysteresis is still present in the 2D model, unlike the 1D model [21]. Thus, the energy

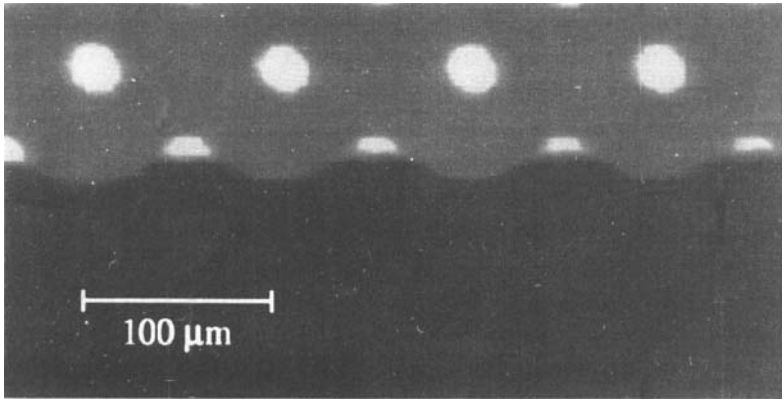

FIGURE 6 CL on a 2D microfabricated array of aluminum dots (bright spots) on a polystyrene surface [43].

in the brokenness of the CL is the key feature of the 2D models just as it must be for ambient surfaces [11,21]. In the 2D models, even for the case of no modulation of the wettability averaged perpendicular to the CL, the amount of hysteresis varies with the surface coverage of the two wettability components. The predicted dependence is very similar to the results seen on an experimental 2D periodic surface [44]. However, the predictions of the model only vaguely describe the observed dependence of hysteresis on experimental models of ambient surfaces (see Section 2.2).

CLJumps: The 2D model explicitly predicts jumps of portions of the CL as the edge of a wettability patch approaches the CL [21]. These jumps are the same size and are temporally and spatially correlated. Uniformity in size and highly correlated jumps have been observed using experimental 2D arrays [43]. However, CL dynamics on ambient surfaces consist of complex jumps with many sizes: for our surfaces from about 1 mm in extent along the CL and about 100 μm perpendicular to the CL down to about micron scale in both directions. The relaxation of one portion of the CL on an ambient surface may induce relaxation of a neighboring portion. Thus, correlation in the jumps is seen only over short distances. Dynamics on ambient surfaces lack the very long length scale correlations present in the 2D models or experiments on 2D arrays of defects.

By accounting for the energy variations in brokenness of the CL, models of wetting on 2D periodic surfaces come closer to wetting behavior on ambient surfaces. In fact, the models clearly describe the CL structure and dynamics on experimental 2D periodic surfaces. However, the very high spatial and temporal correlations in both the 2D models and experiments are not features seen in wetting behavior on ambient surfaces.

3.3. Models with Random Defects

To account for the wettability variations likely to exist on ambient surfaces, various models with random heterogeneity have been developed. We will address four of these models [20,30,45,46]. These models differentiate two regimes: weak heterogeneity where wettability variations from the average are small, $(c_f)_{rms} \ll 1$, and strong heterogeneity where wettability variations from the average are large, $(c_f)_{rms} \sim 1$. The actual wettability variations of a surface are difficult to

determine experimentally (see Section 2.2). Thus, it is difficult to ascertain which regime should be used to treat an experimental surface if the regime is only defined in terms of the variations in the wettability function. Even the condition that CL distortions be smaller than the heterogeneity size [46] is difficult to verify on ambient surfaces. When the restrictions are made in terms of CL structure alone (*e.g.* the slope of the liquid-vapor interface is everywhere much less than $1-$ the small slope approximation that many of the models demand), the experimental observations of CL roughness can provide a clear determination of which theoretical regime should be used.

The four models we discuss approach the problem differently. Joanny and de Gennes treat the mechanics of isolated strong and weak defects and then extend their results to surfaces with dilute, randomly positioned defects [20]. Pomeau and Vannimenus derive a non-linear integral equation for the CL, which they solve in a probabilistic fashion for random, weak heterogeneity patterns on a square lattice [45]. Robbins and Joanny use a random field analysis of the competition between weak heterogeneity and the elasticity of the CL to find the most stable distortions of the CL [30]. Finally, Crassous and Charlaix use Fourier decomposition of the CL and of the wettability function to minimize the energy and determine the Fourier components of a weakly distorted CL [46]. They assume the fundamental wavelength of the CL is equal to the capillary length. In our discussion of 2D models with Fourier decomposition, we suggest that the fundamental wavelength should be the sample size. The larger of the two (capillary length and sample size) would be the most appropriate. When used in these models, the small slope approximation again serves to simplify the elastic energy formulation. In this approximation, a CL distortion of wavelength λ has an elastic energy proportional to $1/\lambda$. The key prediction of the models with weak heterogeneity and with small CL distortions is that even if defects are individually too weak to distort the CL hysteretically, the collective effects of many weak defects can produce hysteresis.

CL Roughness: Robbins and Joanny predict the roughness of a CL distorted by weak heterogeneity to scale as follows [30].

$$w(L) \propto L^{1/2}, \quad L < L_d \tag{11}$$

$$w(L) \propto L^{1/3}, \quad L > L_d \tag{12}$$

$$w(L) \approx \text{constant}, \quad L > a \tag{13}$$

where a is the capillary length and L_d is a characteristic length scale arising from considering the most energetically favorable distortions of the CL. L_d is the minimum length of CL over which the CL distorts from its average position by d, the defect correlation length [30]. The size of CL distortions (reflected in the magnitude of w) can be larger than the defect correlation length because of the cooperative pinning of many defects [30,45]. Thus, large CL distortions on ambient surfaces with only supermolecular scale heterogeneity may arise from cooperative pinning of dense heterogeneity. Eqs. (11) and (12) predict a transition in the scaling behavior of the CL roughness at $L = L_d$. As gravity becomes important on length scales larger than the capillary length, Eq. (13) predicts that the CL roughness is constant above this length scale.

For the CLs we have observed on ambient surfaces, we see neither the 1/2 nor the 1/3 power law exponent (see Section 2.2 and Figure 5). While we sometimes observe flattening of the *w versus L* curve above the capillary length, we often observe continued increase in w to lengths several times the capillary length. However, we must ask whether our surfaces are in the weak heterogeneity regime addressed by this model.

In the elastic energy of the liquid-vapor interface, the models with weak heterogeneity assume small slopes of the liquid-vapor interface (slopes much less than 1) [30,45,46]. We often observe slopes on the order of 1 at the CL, over lengths on the order of 10 μm (see Fig. 2). Thus, our surfaces probably are not in the regime of weak heterogeneity, and discrepancies between the predicted behavior and experimental results may simply be because the surfaces violate the assumptions of the models. Everday experience (e.g. raindrops on windows) often finds CLs with local slopes of order 1. Therefore, many ambient surfaces may not obey the approximations of this class of models.

If adjustments are made to the elastic energy to allow larger liquid-vapor interface slopes, the same theoretical scaling arguments for the distortions of the CL may still arise [47]. Thus, it may still be valid to examine the characteristic length L_d for strong heterogeneity. Since we

observe microscopic CL slopes on the order of 1 over scales on the order of 10 μm, and since we believe the defect correlation length, d, is smaller than 10 μm on our ambient surfaces (so the CL is collectively pinned by multiple defects), then L_d would be on the order of d. From Robbins and Joanny [30].

$$d/L_d \sim [(c_f)_{rms}]^2/\sin^4\theta \tag{14}$$

where θ is the Cassie contact angle. Thus, if $d/L_d \sim 1$ and the contact angle is not too small, then $(c_f)_{rms} \sim 1$. This confirms that our surfaces have strong heterogeneity.

The CL roughness on our experimental surfaces is not accurately described by these models. Perhaps, these and other ambient surfaces do not comply with the assumptions of the models. However, the models do provide criteria to ascertain whether a surface has strong or weak heterogeneity by examination of the magnitude of slopes along the CL.

Hysteresis Versus Surface Coverage: These models examine the dependence of the hysteresis on the density of defects [20,46]. A single defect is predicted to distort the CL hysteretically only of the defect strength is above a critical value [20,46]. For multiple, non-interacting defects (*i.e.*, the distortion of the CL by one defect does not affect the shape of the distortion at a neighboring defect in more than a mean field, or average, manner), this same critical defect strength is needed to produce hysteresis. If the defects do interact, then the critical defect strength needed for the cooperating defects to distort the CL hysteretically decreases as the defect density grows. Thus, multiple, weak defects can cause hysteresis even if a single defect acting alone could not.

Hysteresis is predicted to increase with increasing defect density [20,46]. For isolated defects, the increase is linear with the defect density [20,46]. For interacting defects, hysteresis increases with a power law exponent of 0.7 [46]. The results of Crassous and Charlaix can be compared to the exponents of 0.4 and 0.8 (depending on the defect size) found in experiments [37]. The disagreement between the model and the experiments may arise due to the fact that the defect size and defect densities in the experiments were not in the regimes addressed by the model.

CL Jumps: The model employing the random field techniques predicts that the smallest jumps of the CL for quasistatic motion should be L_d by d [47]. If one can argue, as we did above, that a characteristic length L_d still exists in the regime of strong heterogeneity, we can estimate L_d and d by examining the microscopic jumps of the CL in our experiments. We observe jumps of the CL at least down to the order of microns. This puts an upper bound on both L_d and d of about $1-10\,\mu m$ for our experimental ambient surfaces. Observations of jump sizes on other ambient surfaces could provide similar information about these length scales for those surfaces.

4. VIBRATIONS AND TIME SCALES

Mechanical vibrations affect contact angles on heterogeneous surfaces [4–6, 12, 39–41] and cause the angles to exhibit a time dependence [6]. The microscopic distortions of a CL on an ambient surface are caught in metastable states bounded by energy barriers. Thermal energies are insufficient to overcome these barriers and relax the CL in finite time. However, vibrations can overcome the energy barriers and relax the distortions of a CL in experimentally accessible times. The relaxation of the microscopic structure of the CL by vibrations causes the macroscopically-averaged contact angle to depend on the vibration level. Influence of vibrational noise on contact angles has long been qualitatively discussed [12, 39–41]. Experimental studies have shown that vibrations can relax contact angles and partially or completely mitigate hysteresis [4–6]. In addition, not only the amount of relaxation, but also the rate of relaxation depends on the vibrational noise level [6]. Thus, a complete quantitative modeling and correct interpretation of contact angle hysteresis must include the time scale of the measurement relative to the time scale of the vibrations.

We can describe the different time scales in contact angle hysteresis by considering the experiment where a vertical, partially-immersed plate is moved up and down in a liquid bath. The period of the plate cycle, T, sets the time scale of CL motion and the time available for the contact angle to move between its advance and recede values. In other experiments, T may represent the time of the measurement process itself. We have observed that vibrations can relax the contact

angle with a relaxation time, τ, which depends on the vibration level (Fig. 7). On the heterogeneous surfaces we have examined, vibration levels needed to relax contact angles significantly occur in typical experimental environments and the time scales over which the angles relax are relevant in typical contact angle experiments. The time scale of the vibration level and the time scale of CL motion together control the amount of hysteresis. When $\tau \gg T$, the CL moves between advance and recede conditions before the CL can relax completely due to vibrations. When $\tau < T$, the CL speed is slow enough that vibrations of a given level can relax the contact angle. Hysteresis may or may not be mitigated in this regime depending on the vibration level. In this regime, measurements give contact angles which are relaxed and controlled by vibrations in the experimental environment. As the CL speed goes to zero and T becomes infinite, thermal noise will eventually (over experimentally inaccessible times) relax the contact angle and mitigate hysteresis on ambient surfaces. As surfaces become more homogeneous, the energy barriers can become smaller; and thermal relaxation becomes important. As the limit of homogeneity on the scale of thermal fluctuations of the liquid-vapor interface is approached,

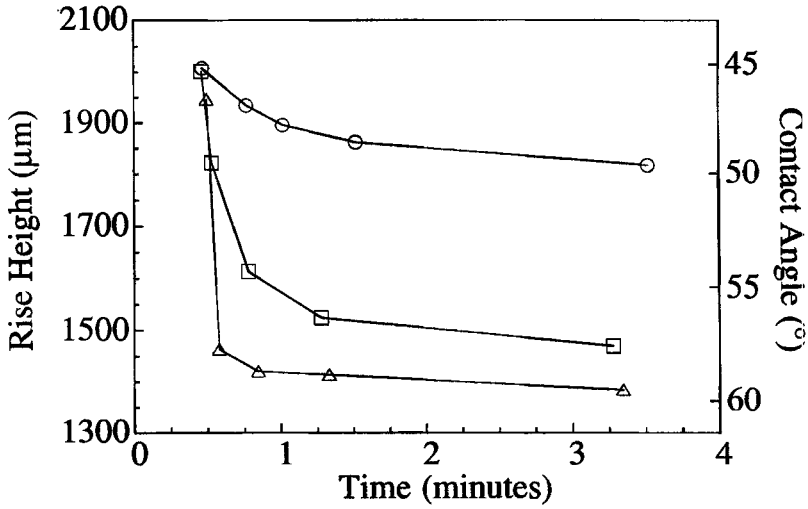

FIGURE 7 Relaxation of macroscopically-averaged recede contact angle for three vibration amplitudes of: ○ – 0.1a, □ – 0.2a, and Δ – 0.4a. (a = capillary length = 2.7 mm).

energy dissipation due to the fluctuations in the CL disappears and the macroscopic contact angle hysteresis (due to surface heterogeneity) becomes negligible. Thus, a complete, quantitative description of contact angle hysteresis must account for the effects of vibrations with the appropriate description of temporal scales. In addition, the model must describe the transition to thermal relaxation and the disappearance of hysteresis as surfaces approach homogeneity down to the molecular scale.

5. SUMMARY

Causing drops to be retained on surfaces or in capillary tubes, contact angle hysteresis is ubiquitous in nature and technology. Contact angles are used to characterize the average and spatial variations in the chemistry of surfaces. Quantitative models of contact angle hysteresis are needed to engineer surfaces which shed or retain drops and to interpret contact angle measurements.

Due to their natural physical roughness and chemical heterogeneity, ambient surfaces have strongly varying wettability. CLs on ambient surfaces are rough on many length scales. On typical experimental realizations of ambient surfaces, distortions of the CL extend at least down to scales on the order of 1 μm along the CL. The distortions can be larger (perpendicular to the CL) than the scale of the heterogeneity variation. Some distortions extend across lengths (parallel to the CL) longer than the capillary length. Clearly, collective pinning across many sites of heterogeneity is common. When the CL is forced to move slowly across the surface, the CL exhibits jumps down to micron scale with coupling between the motion of neighboring points on the CL. Reproducibility of CL configurations [6, 38] and slopes of the CL on the order of 1 indicate that ambient surfaces probably exhibit strong pinning, *i.e.* local wettability variations strongly distort the CL.

Models of wetting on heterogeneous surfaces have treated surfaces with ever more complex wettability variations. The first 1D models of heterogeneous surfaces, with a wettability modulation only perpendicular to the CL, set the basic principles and show the qualitative behavior of hysteresis including metastable states that can pin the CL. The 2D models demonstrate that hysteresis results even without

modulation of the wettability averaged perpendicular to the CL, a characteristic of ambient surface. Thus, the contribution to the energy functional from the distortion of the CL is the important key to hysteretic behavior of ambient surfaces. Care must be used in interpreting quantitative results of both theoretical and experimental models on ordered arrays of defects. The highly correlated CL structure and jumps in these models and experiments mask important aspects of wetting on surfaces with more random wettability. Models with random wettability focus mainly on the case of weak heterogeneity. They show the cooperative behavior that can produce hysteresis from weak defects which individually could not hysteretically distort the CL. These models predict a power law scaling for the roughness of the CL. However, their applicability to the strong pinning on ambient surfaces is in doubt. Quantitative descriptions of wetting on ambient surfaces will have to deal with the limit of dense, strongly-pinning heterogeneity.

While progress has been made, a quantitative description of contact angle hysteresis on ambient surfaces is not yet available. Such a model of contact angle hysteresis needs to account for not only the spatial characteristics of wetting on ambient surfaces, but also the relevant time scales. Modeling has addressed neither the strong influence of vibrations on contact angle hystersis in typical experimental environments nor contact angle relaxation over experimentally relevant time scales.

Acknowledgements

We are grateful for discussions with M. O. Robbins and for support from NSF grant DMR-9411900.

References

[1] de Gennes, P. G., *Rev. Mod. Phys.* **57**, 289 (1985).
[2] Good, R. J., *J. Adhesion Sci. Technol.* **6**, 1269 (1992).
[3] Schrader, M. E. and Loeb, G. I., Eds., *Modern Approaches to Wettability: Theory and Applications* (Plenum, New York, 1992).
[4] Smith, T. and Lindberg, G., *J. Colloid Interface Sci.* **66**, 363 (1978).
[5] Andrieu, C., Sykes, C. and Brochard, F., *Langmuir* **10**, 2077 (1994).
[6] Decker, E. L. and Garoff, S., *Langmuir* **12**, 2100 (1996).
[7] Dussan V., E. B. and Chow, R. T.-P., *J. Fluid Mech.* **137**, 1 (1983).
[8] Dussan V., E. B., *J. Fluid Mech.* **151**, 1 (1985).

[9] Dussan V., E. B., *J. Fluid Mech.* **174**, 381 (1987).
[10] Collins, R. E., *Flow of Fluids Through Porous Media* (Reinhold, New York, 1961), Chap. 2.
[11] Good, R. J., *J. Amer. Chem. Soc.* **74**, 5041 (1952).
[12] Johnson, R. E., Jr. and Dettre, R. H., "Wettability and Contact Angles," in *Surface and Colloid Science*, Matijevic, E., Ed. (Wiley, New York, 1969), Vol. 2, pp. 85–153.
[13] Neumann, A. W. and Good, R. J., *J. Colloid Interface Sci.* **38**, 341 (1972).
[14] Eick, J. D., Good, R. J. and Neumann, A. W., *J. Colloid Interface Sci.* **53**, 235 (1975).
[15] Timmons, C. O. and Zisman, W. A., *J. Colloid Interface Sci.* **22**, 165 (1966).
[16] Martynov, G. A., Starov, V. M. and Churaev, N. V., *Colloid J. USSR* **39**, 406 (1977).
[17] Schwartz, A. M., *J. Colloid Interface Sci.* **75**, 404 (1980).
[18] Neumann, A. W. and Good, R. J., "Techniques of Measuring Contact Angles," in *Surface and Colloid Science*, Good, R. J. and Stromberg, R. R., Eds. (Wiley, New York, 1969), Vol. 11, pp. 31–91.
[19] Dussan, V., E. B., Ramé, E. and Garoff, S., *J. Fluid Mech.* **230**, 97 (1991).
[20] Joanny, J. F. and de Gennes, P. G., *J. Chem. Phys.* **81**, 552 (1984).
[21] Schwartz, L. W. and Garoff, S., *Langmuir* **1**, 219 (1985).
[22] Everett, D. H. and Whitton, W. I., *Faraday Soc. Trans.* **48**, 749 (1952).
[23] Everett, D. H. and Smith, F. W., *Faraday Soc. Trans.* **50**, 187 (1954).
[24] Everett, D. H., *Faraday Soc. Trans.* **50**, 1077 (1954).
[25] Kumar, A. and Whitesides, G. M., *Appl. Phys. Lett.* **63**, 2002 (1993).
[26] Kumar, A., Biebuyck, H. A. and Whitesides, G. M., *Langmuir* **10**, 1498 (1994).
[27] Frank, B., Ph.D. Thesis, *Surfactant Self-Assembly Near Contact Lines: Control of Advancing Surfactant Solutions*, Carnegie Mellon University, Pittsburgh, PA, (1995), p. 104.
[28] Frank, B. and Garoff, S., *Langmuir* **11**, 4333 (1995).
[29] Cassie, A. B. D., *Discuss. Faraday Soc.* **3**, 11 (1948).
[30] Robbins, M. O. and Joanny, J. F., *Europhys. Lett.* **3**, 729 (1987).
[31] Garoff, S., Hall, R. B., Deckman, H. W. and Alvarez, M. S., "Molecular Aspects of Wetting on Surfactant Coated Surfaces," in *Chemistry and Physics of Composite Media*, Tomkiewicz, M. and Sen, P. N., Eds. (Electrochem. Soc. Inc., Pennington, NJ, 1985), p. 112.
[32] Ulman, A., Evans, S. D., Shnidman, Y., Sharma, R. and Eilers, J. E., *Adv. Colloid Interface Sci.* **39**, 175 (1992), and references therein.
[33] Bain, C. D. and Whitesides, G. M., *J. Am. Chem. Soc.* **110**, 6560.
[34] Bain, C. D., Evall, J. and Whitesides, G. M., *J. Am. Chem. Soc.* **111**, 7155 (1989).
[35] Ulman, A., Evans, S. D., Shnidman, Y., Sharma, R., Eilers, J. E. and Chang, J. C. *J. Am. Chem. Soc.* **113**, 1499 (1991).
[36] Stranick, S. J., Parikh, A. N., Tao, Y.-T., Allara, D. L. and Weiss, P. S., *J. Phys. Chem.* **98**, 7636 (1994).
[37] di Meglio, J.-M., *Europhys. Lett.* **17**, 607 (1992).
[38] Nadkarni, G. D. and Garoff, S., *Langmuir* **10**, 1618 (1994).
[39] Schwartz, L. W. and Garoff, S., *J. Colloid Interface Sci.* **106**, 422 (1985).
[40] Li, D. and Neumann, A. W., *Colloid Polym. Sci.* **270**, 498 (1992).
[41] Marmur, A., *J. Colloid Interface Sci.* **168**, 40 (1994).
[42] Joanny, J. F. and Robbins, M. O., *J. Chem. Phys.* **92**, 3206 (1990).
[43] Nadkarni, G. D., Ph.D. Thesis, *The Complex Microscopic Contact Line Motion on Ambient Surfaces*, Carnegie Mellon University, Pittsburgh, PA (1993).
[44] de Jonghe, V. and Chatain, D., *Acta Metall. Mater.* **43**, 1505 (1995).
[45] Pomeau, Y. and Vannimenus, J., *J. Colloid Interface Sci.* **104**, 477 (1985).
[46] Crassous, J. and Charlaix, E., *Europhys. Lett.* **28**, 415 (1994).
[47] Robbins, M. O., private communication.